RSC Advances

PAPER

View Article Online
View Journal | View Issue

Cite this: *RSC Adv.*, 2017, **7**, 6994

Formation and conversion of six temperature-dependent fluorescent Zn^{II}-complexes containing two *in situ* formed N-rich heterocyclic ligands†

Qin Wei,[a] Mei-Juan Wei,[a] Yan-Jun Ou,[a] Ji-Yuan Zhang,[d] Xia Huang,[a] Yue-Peng Cai*[abc] and Li-Ping Si*[a]

Received 23rd October 2016
Accepted 13th January 2017

DOI: 10.1039/c6ra25678c

www.rsc.org/advances

Six temperature-dependent Zn(II) complexes **1–6** based on the simple Schiff base L^1 from condensation of equivalent 2-pyridine formaldehyde (2-Pfd) and 2-pyridylethylamine (2-Pea) were systematically studied for the first time. These six complexes are: two complexes of ZnL^2X_2 (**1** and **2**) involving *in situ* formed N-rich heterocyclic ligand L^2 at 80 °C; two complexes of $[Zn_2(cis\text{-}L^3)X_4\cdot S]$ (S = H_2O for **3**, S = 0 for **5**) involving *in situ* formed azaheterocyclic ligand *cis*-L^3 at 100 °C; and the rest two ones of $[[Zn_2(trans\text{-}L^3)X_4]$ (**4** and **6**) involving *in situ* formed azaheterocyclic ligand *trans*-L^3 at 120 °C (where X = Cl (**1**, **3**, **4**) and N_3 (**2**, **5**, **6**), L^1 = *N*-(2-pyridylmethyl)-pyridine-2-carbaldimine, L^2 = 1-pyridineimidazo-[1,5-*a*]pyridine, L^3 = 1-(1,2-di(pyridin-2-yl)-2-(3-(pyridin-2-yl)*H*-imidazo-[1,5-*a*]-pyridin-1-yl)-ethyl)-3-(pyridin-2-yl)*H*-imidazo-[1,5-*a*]pyridine). Interestingly, three Cl-based complexes **1**, **3**, **4** under appropriate conditions can be irreversibly translated into the corresponding N_3-based **2**, **5**, **6**, respectively. The possible formation/conversion mechanism shows that the α-H activation in –CH=N–CH_2– moiety of L^1 coordinated to Zn^{2+} ion should be the original driving force for the intermolecular C–C/C–N coupling and ring formation reactions, meanwhile reaction temperature also plays a very important role during the formation/conversion of **1–6**. Moreover, the results indicate that complexes **1–6** have good fluorescence properties as potential fluorescent materials.

Introduction

The C–H bond in the α-position to an imino group –CH=N–CH_2– is activated after the imino nitrogen atom is coordinated to a metal center.[1] Basic acceptors, such as pyridine, imidazole, *etc.*, have the ability to deprotonate the imino carbon-bound hydrogen atom to form 1,3-dipole. According to the classification of Huisgen, the 1,3-dipole of $C{=}N^+{-}C^-$ can be represented as $X{=}Y^+{-}Z^-$ of allylic type.[2] Schiff base *N*-(2-pyridylmethyl)-pyridine-2-carbaldimine (L^1) with bipyridyl groups, condensed from equivalent 2-pyridine formaldehyde (2-Pfd) and 2-pyridylethylamine (2-Pea), may be led to various N-rich heterocyclic products under the guidance of the metal ion coordination induced effect, *e.g.* titanium(III), iron(II) and nickel(II) complexes containing 2,3,5,6-tetra-(pyridin-2-yl)piperazine/pyrrole[3] as well as cadmium(II) complexes with 2,2′,2″-(1-(pyridin-2-ylmethyl)imidazolidine-2,4,5-triyl)tripyridine[4] are typical examples of such products.

Obviously, *in situ* formation of these N-rich heterocycles and their derivatives is very important in various fields: (i) azaheterocycles in organic syntheses can act as protective groups, since they are particularly easy to hydrolyze in acidic solutions and are stable in basic solutions. (ii) Some azaheterocycles can be used as intermediates in the biosynthesis of nucleotides, avoiding the shortcomings of traditional synthesis methods, and some of their metal complexes are found to be active as cytotoxic metallopharmaceuticals.[5] (iii) They are important building blocks in biologically active compounds and carriers of pharmacologically active carbonyl compounds, and some of metal complexes are potential chemotherapeutic agents for DNA cleavage.[6] (iv) Their transition-metal complexes have been also extensively studied for applications in OLEDs, luminescent materials,[7] *etc.* Hence, it is very meaningful to explore the formation conditions and coordination behaviors of multi-substituted N-rich heterocycles by solvothermal *in situ* metal-induced reaction from simple Schiff base ligands. Herein we report the syntheses and their subsequent coordination

[a]*School of Chemistry and Environment, South China Normal University, P. R. China. E-mail: caiyp@scnu.edu.cn*

[b]*Guangzhou Key Laboratory of Materials for Energy Conversion and Storage, Guangzhou 510006, P. R. China*

[c]*Guangdong Provincial Engineering Technology Research Center for Materials for Energy Conversion and Storage, Guangzhou 510080, P. R. China*

[d]*Guangzhou Institute of Energy Conversion, Chinese Academy of Sciences, Guangzhou 510640, P. R. China*

† Electronic supplementary information (ESI) available: The TGA curves, liquid-state emission as well as the related UV absorption spectra at 100 °C and 120 °C, XRD patterns of compounds **1–6**; and Tables S1–S3 of selected bond lengths, bond angles, hydrogen bonds, crystal data and structure refinement, as well as X-ray crystallographic files in CIF format for six compounds **1–6** are available in ESI. CCDC 1032239, 1508822, 1032241, 1508812, 1032243 and 1032244 for **1–6**, respectively. For ESI and crystallographic data in CIF or other electronic format see DOI: 10.1039/c6ra25678c

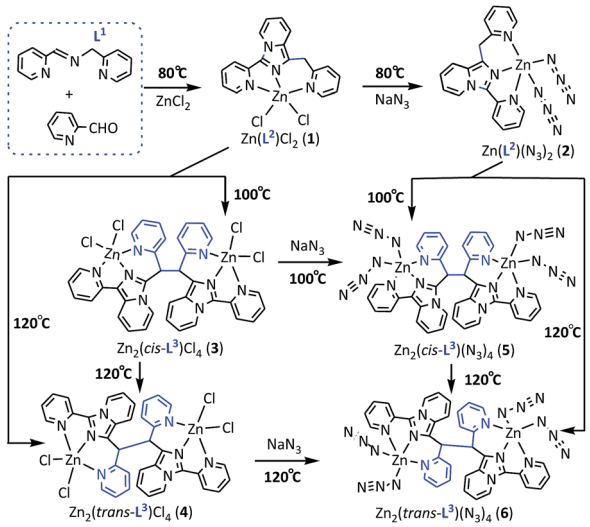

Scheme 1 The formation and conversion of six temperature-dependent Zn(II)-complexes containing *in situ* forming azaheterocycles L^2/L^3 from pyridine-type Schiff base L^1 mediated by Zn^{2+} ion.

chemistry of two imidazo[1,5-*a*]-pyridine-based azahetero-cycles involving 2-pyridine bis/tetra-substitutents(L^2/L^3), produced from zinc(II)-mediated inter-molecular ring-forming and C–C coupling reactions of L^1 in the presence of another equimolar 2-Pfd under different reaction temperatures (Scheme 1), in which six new resulted Zn^{II} coordination polymers, namely ZnL^2Cl_2 (**1**), $ZnL^2(N_3)_2$ (**2**).

$Zn_2(cis\text{-}L^3)Cl_4\cdot H_2O$ (**3**), $Zn_2(trans\text{-}L^3)Cl_4$ (**4**), $Zn_2(cis\text{-}L^3)(N_3)_4$ (**5**) and $Zn_2(trans\text{-}L^3)(N_3)_4$ (**6**) (L^1 = *N*-(2-pyridyl-methyl)pyridine-2-carbaldimine, L^2 = 1-pyridine-imidazo-[1,5-*a*]pyridine, L^3 = 1-(1,2-di-(pyridin-2-yl)-2-(3-(pyridin-2-yl)*H*-imidazo[1,5-*a*]-pyridin-1-yl)eth-yl)-3-(pyridin-2-yl)*H*-imidazo[1,5-*a*]pyridine), are involved. To the best of our knowledge, this is the first example that Zn^{2+}-mediated C–C/C–N bond-forming strategy toward bis/tetra-substituted aza-heterocycles *in situ* from simple pyridine-type Schiff base.

Experimental section

Materials and methods

All reagent were grade obtained from commercial sources and used without further purification. Solvents were dried by the standard procedures. Elemental analyses for C, H, N were performed on a Perkin-Elmer 240C analytical instrument. IR spectra were recorded on a Nicolet FT-IR-170SX spectro-photometer in KBr pellets. Thermogravimetric analyses were performed on Perkin-Elmer TGA7 analyzer with a heating rate of 10 °C min^{-1} in flowing air atmosphere. The solid state luminescent spectra were recorded at room temperature on Hitachi F-2500 and Edinburgh-FLS-920 with a xenon arc lamp as the light source. In the measurements of emission and excitation spectra the pass width is 5.0 nm. X-ray powder diffraction patterns were measured on a Bruker D8 Advance diffractometer at 40 kV and 40 mA with a Cu target tube and a graphite monochromator. Nitrogen and hydrogen adsorption isotherms were taken on a Belsorp-Max surface area and pore size analyzer.

Synthesis of L^1

For complexes **1–6**, they were prepared by a similar procedure except reaction temperature and auxiliary ligand NaN_3. A mixture of *N*-(2-pyridylmethyl)pyridine-2-carbaldimine (L^1) (0.0394 g, 0.2 mmol), $ZnCl_2$ (0.0402 g, 0.2 mmol), 2-pyridine formaldehyde (0.022 g, 0.2 mmol), DMF (7 mL) and pyridine (3 mL) was sealed in a 15 mL Pyrex tube. The tube was heated for 3 days under autogenous pressure, and then slowly cooled the reaction solution to room temperature over 24 h and filtered to give pale yellow block single crystals for 1 at 80 °C, 3 at 100 °C and 4 at 120 °C. When NaN_3 (0.130 g, 0.4 mmol) was added to the collected filtrate, three new complexes **2** (80 °C), **5** (100 °C) and **6** (120 °C) were obtained under the same reaction conditions, respectively. The crystals were collected by filtration, washed with Et_2O (2 × 3 mL), and dried in air (Table 1).

Syntheses of complexes 1–6

ZnL^2Cl_2 (1). Yield: 75% (based on Zn). Elemental analysis calcd (%) for $C_{18}H_{14}ZnCl_2N_4$: C, 51.11; H, 3.31; N, 13.25. Found: C, 51.07; H, 3.36; N, 13.27. IR frequencies (KBr, cm^{-1}): 3562–3443(br, s), 2959(w), 2370(w), 1635(m), 1596(s), 1561(s), 1486(m), 1419(s), 1376(w), 1340(m), 1252(w), 1171(m), 1073(w), 1002(w), 847(w), 782(m), 763(w), 682(m), 635(w), 519(w), 467(w).

$ZnL^2(N_3)_2$ (2). Yield: 69% (based on Zn). Elemental analysis calcd (%) for $C_{18}H_{14}ZnN_{10}$: C, 49.57; H, 3.21; N, 32.13. Found: C, 49.59; H, 3.24; N, 32.09. IR frequencies (KBr, cm^{-1}): 3563–3448(br, s), 2995(m), 2892(s), 2798(s), 2063(m), 1635(vs), 1597(m), 1540(s), 1470(vs), 1445(s), 1342(vs), 1291(s), 1188(vs), 1151(s), 1022(s), 902(vs), 793(s), 763(m), 675(m), 637(m), 601(w), 572(m), 529(m), 463(w).

$Zn_2(cis\text{-}L^3)Cl_4\cdot H_2O$ (3). Yield 75% (based on Zn). Elemental analysis calcd (%) for $C_{36}H_{28}Zn_2Cl_4N_8O$: C, 50.16; H, 3.25; N, 13.01. Found: C, 50.18; H, 3.27; N, 13.05. IR frequencies (KBr, cm^{-1}): 3561–3433(s,br), 2955(m), 2372(s), 2051(m), 1639(s), 1574(s), 1421(s), 1335(s), 1259(w), 1193(w), 1154(m), 1006(m), 923(w), 879(w), 777(s), 646(w), 620(m), 564(w), 515(m).

$Zn_2(trans\text{-}L^3)Cl_4$ (4). Yield 67% (based on Zn). Elemental analysis calcd (%) for $C_{36}H_{26}Zn_2Cl_4N_8$: C, 51.23; H, 3.08; N, 13.28. Found: C, 51.19; H, 3.11; N, 13.33. IR frequencies (KBr, cm^{-1}): 3565–3443(br,s), 2994(m), 2887(m), 2796(s), 2045(m), 1634(s), 1598(vs), 1540(s), 1471(s), 1444(vs), 1347(m), 1290(vs), 1187(s), 1150(vs), 1023(s), 902(s), 794(m), 764(s), 678(m), 635(m), 603(m), 574(w), 525(m), 464(w).

$Zn_2(cis\text{-}L^3)(N_3)_4$ (5). Yield 73% (based on Zn). Elemental analysis calcd (%) for $C_{36}H_{26}Zn_2N_{20}$: C, 49.68; H, 2.99; N, 32.20. Found: C, 49.65; H, 3.03; N, 32.25. IR frequencies (KBr, cm^{-1}): 3567–3447(br, s), 2956(w), 2366(w), 2062(m), 1649(s), 1561(m), 1523(w), 1482(m), 1433(s), 1341(s), 1259(w), 1151(m), 1012(m), 975(w), 879(w), 844(w), 780(m), 720(m), 651(w), 518(m), 460(w).

$Zn_2(trans\text{-}L^3)(N_3)_4$ (6). Yield 70% (based on Zn). Elemental analysis calcd (%) for $C_{36}H_{26}Zn_2N_{20}$: C, 49.68; H, 2.99; N, 32.20. Found: C, 49.70; H, 3.03; N, 32.22. IR frequencies (KBr, cm^{-1}): 3566–3446(br, s), 2996(s), 2893(m), 2798(s), 2061(m), 1636(s),

Table 1 Crystallographic data and structure refinement summary for **1–6**

Complex	**1**	**2**	**3**	**4**	**5**	**6**
Empirical formula	$C_{18}H_{14}Cl_2N_4Zn$	$C_{18}H_{14}N_{10}Zn$	$C_{36}H_{28}Cl_4N_8OZn_2$	$C_{36}H_{26}Cl_4N_8Zn_2$	$C_{36}H_{26}N_{20}Zn_2$	$C_{36}H_{26}N_{20}Zn_2$
Formula weight	422.60	435.76	1246.63	843.19	869.51	869.51
Crystal system	Monoclinic	Monoclinic	Monoclinic	Monoclinic	Monoclinic	Triclinic
Space group	$P2_1/n$	$C2/c$	$P2_1/c$	$P2_1/c$	$P2_1/n$	$P\bar{1}$
a (Å)	7.229(3)	18.130(3)	15.388(6)	8.730(2)	8.884(2)	8.0218(8)
b (Å)	14.023(6)	18.615(3)	12.271(5)	13.047(4)	19.730(5)	10.0798(10)
c (Å)	19.027(7)	13.827(2)	19.046(6)	15.560(4)	21.404(6)	11.6154(12)
α (°)	90	90	90	90	90	83.9840(10)
β (°)	95.403(5)	128.341(2)	122.12(2)	96.344(3)	93.623(4)	83.1740(10)
γ (°)	90	90	90	90	90	76.6970(10)
V (Å^3)	1920.3(13)	3660.1(10)	3046.0(2)	1761.5(8)	3744.1(18)	904.60(16)
Z	4	8	2	2	4	1
ρ(cald.) (mg m^{-3})	1.462	1.582	1.359	1.590	1.543	1.596
T (K)	298(2)	293(2)	298(2)	296(2)	296(2)	296(2)
μ (mm^{-1})	1.564	1.371	0.688	1.705	1.340	1.386
R_{int}	0.0355	0.0395	0.0543	0.0298	0.0672	0.0168
GOF	1.027	1.021	1.040	1.052	1.050	1.032
R_1 [$I > 2\sigma(I)$][a]	0.0320	0.0455	0.0491	0.0395	0.0600	0.0483
wR_2 (all data)[b]	0.0748	0.1137	0.1328	0.1007	0.1514	0.1387

[a] $R_1 = \sum||F_o| - |F_c||/\sum|F_o|$. [b] $wR_2 = \{\sum[w(F_o^2 - F_c^2)^2]/\sum(F_o^2)^2\}^{1/2}$, where $w = 1/(\sigma^2(F_o^2) + (aP)^2 + bP)$, $P = (F_o^2 + 2F_c^2)/3$.

1598(vs), 1543(s), 1474(s), 1450(s), 1342(vs), 1295(s), 1193(vs), 1153(m), 1026(s), 897(vs), 796(m), 764(s), 680(m), 644(m), 599(m), 568(m), 529(m), 468(w).

Alternatively, two N_3-based complexes **5, 6** can be also obtained *via* stirring reactions from NaN_3 and the corresponding Cl-based complexes **1**, **3** and **4** for 5 hours at 100 and 120 °C, respectively.

X-ray crystallographic studies

Complexes **1–6** were characterized by single crystal X-ray diffraction. Suitable single crystals were mounted on a glass fiber and the intensity data were collected on a Bruker APEX II diffractometer at 298 K using graphite monochromatic Mo-Kα radiation ($\lambda = 0.71073$ Å). Absorption corrections were applied using the multi-scan program SADABS.[8] Structural solutions and full-matrix least-squares refinements based on F^2 were performed with the SHELXS-97 (ref. 9) and SHELXL-97 (ref. 10) program packages, respectively. All non-hydrogen atoms were refined with anisotropic displacement parameters. Hydrogen atoms on organic ligands were generated by the riding mode (C–H 0.96 Å). For **1** and **3**, the SQUEEZE option in PLATON[11] was used to remove the disordered solvent water molecules, and the actual water molecules in the unit cell are determined by elemental and thermo-gravimetric analyses (EA and TGA). A summary of the parameters for the data collection and refinements for nine complexes are given in Table S1.† Selected bond lengths and angles for complexes **1–6** are listed in Table S2.† Hydrogen bond lengths and angles for complex **3** are given in Table S3.† CCDC reference numbers for **1–6** are CCDC 1032239, 1508822, 1032241, 1508812, 1032243 and 1032244, respectively.

Results and discussion

Syntheses and general characterization of complexes

Pale-yellow crystals of **1–6** (*ca.* 67–75% yield) were obtained from the *in situ* solvothermal treatment of *N*-(2-pyridylmethyl)-pyridine-2-carbaldimine (L^1) with $ZnCl_2/ZnCl_2 + NaN_3$ in the mixed solvents of DMF and pyridine (v/v = 2 : 1) at 80–120 °C for three days (see Scheme 1). The component diversification of the resulting discrete Zn^{II}–L^{1-3} complexes **1–6** can be tuned simply by changing reaction temperature, in which *in situ* forming L^2/L^3 are the results of intermolecular C–C/C–N coupling and ring-forming reactions deriving from α-H activation at *ortho*-position of imine –CH=N–CH_2– moiety reduced by Zn(II) coordination (possible *in situ* forming mechanism in Scheme S1†). Elemental analysis and PXRD (Fig. S1 in the ESI†) confirmed the phase purity of the bulk materials. Compounds **1–6** are air-stable and insoluble in water and most organic solvents. Meanwhile, stirring reactions of NaN_3 and the Cl-based complexes **1**, **3** and **4** for 5 hours at 100 °C and 120 °C can irreversibly convert into corresponding N_3-based complexes **5** and **6** in high yield, respectively. Or alternatively the direct reaction of L1 with $ZnCl_2$ + NaN_3 like the Cl-based complexes **1**, **3** and **4** can also give the corresponding N_3-based complexes **2**, **5** and **6**. However, they are not only low yield, but also difficult to isolate and purify. This probably stems from the diverse coordination modes of azide anion (such as η^1-, μ(1,1)- and μ(1,3)-modes, *etc.*), especially under high temperature conditions. In contrast, azide substitution reactions based on Cl-based zinc complexes, due to a single final product, have obvious advantages.

In the IR spectra of six compounds **1–6**, the strong bands in the region of 3443–3567 cm^{-1} or so are due to a hydrogen bonding C–H···Cl(N) interactions. The strong C=N bands occurring in the range of 1597–1635 cm^{-1} for these complexes are shifted considerably toward lower frequencies compared to that of the free Schiff base ligand L1 (1646 cm^{-1}), showing that the azomethine nitrogen atom is coordinated to the metal.[12] The weak bands in the region of 462–467 cm^{-1} for the six complexes can be assigned to ν(M–N/Cl),[12] and provides further evidence for the coordination was through the terminal nitrogen/chlorine atoms. The position of the 2061–2063 cm^{-1} (ν_{as}-N_3) falls within the absorption range of terminal azides in

transition metal complexes,[13] and the appearance of the ν_s-N_3 band at 1341–1342 cm^{-1} indicates the asymmetric nature of the azide groups in three complexes **2**, **5**, **6**.

Thermal stability of six complexes was investigated by the TGA technique (see Fig. S2†). The TG curve for **3** shows two steps of weight loss. The weight loss of the uncoordinated water molecules is observed from 83 to 112 °C for **3** (calc. 2.09% and exp. 1.96%). On further heating, the complexes start to be decomposed at 312 °C for **3**. For the remaining five complexes **1**, **2**, **4**, **5** and **6**, their TGA curves are also similar and present one step of weight loss, namely decomposition of the complexes are observed at 205 °C for **1**, 321 °C for **2**, 307 °C for **4**, 341 °C for **5** and 343 °C for **6**, respectively. Although all six complexes are zero dimensional, their thermal stability is obviously different, probably due to the different dimensions of their supramolecular structures, in which the complex **3** has low dimensional (2D) supramolecular structure and shows the lowest thermal stability (see below for details).

Structural analysis and discussion

ZnL^2Cl_2 (1). When the reaction of ligand L^1 with an equimolar amount of 2-pyridine formaldehyde and $ZnCl_2$ at 80 °C lasted for three days, 0-D compound **1** was obtained. Its asymmetric unit involves one crystallographically independent mononuclear molecule ZnL^2Cl_2 (Fig. 1), and each molecule has an essentially undistorted square pyramidal coordination geometry around the zinc(II) ion satisfied by three nitrogen atoms (N1, N2, N3) from *in situ* formed ligand L^2 and two terminal coordinated chlorine atoms (Cl1, Cl2). The Zn–N bond length of (2.030(4)–2.385(4) Å), and Zn–Cl (2.2602(14)–2.2626(16) Å) bond distances are in the expected range for this coordination geometry with zinc(II). The ligand L^2 shows μ_1-η^1:η^1:η^1 coordination mode. Due to intermolecular hydrogen bonding C–H···Cl and π···π packing interactions (Table S3†), a 2-D supramolecular layer-like structure with 4^4 topology is assembled and as indicated in Fig. 2.

$ZnL^2(N_3)_2$ (2). When NaN_3 is added to the reaction mixture, two coordinated chlorine atoms in **1** are replaced by two azide ions and produce a new complex $ZnL^2(N_3)_2$ (**2**) (Fig. 3) at the same reaction temperature. Similar to **1**, complex **2** is also a 0-D mononuclear structure, and its asymmetric unit involves one.

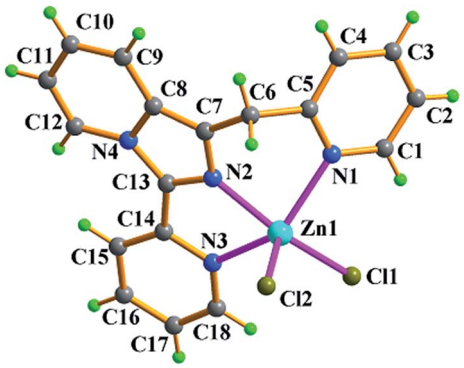

Fig. 1 Molecular structure of compound ZnL^2Cl_2 (**1**) with atomic labels.

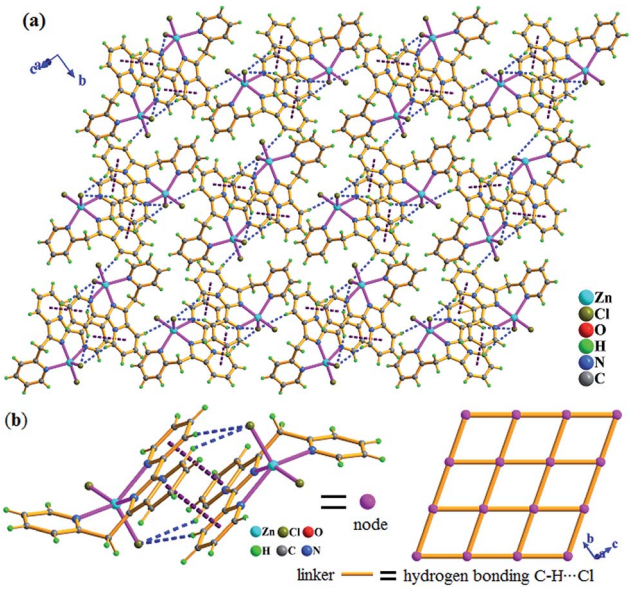

Fig. 2 In **1**, (a) 2-D supramolecular layer assembled by intermolecular hydrogen bonding C–H···Cl (blue color) and π···π packing (violet color) interactions in *bc* plane. (b) 4^4 topological supramolecular layer, in which the dimmer unit $(ZnL^2Cl_2)_2$ as node constructed by intermolecular C–H···Cl and π···π packing interactions, interunit hydrogen bond C–H···Cl as linker.

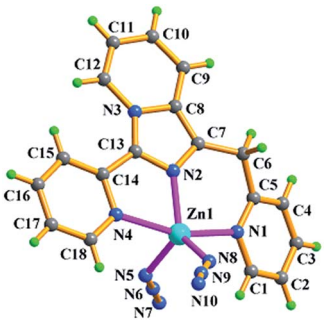

Fig. 3 Molecular structure of $ZnL^2(N_3)_2$ (**2**) with atomic labels.

Zn^{2+} ion, one *in situ* formed L^2 ligand, and two terminal monodentate η^1-coordinated N_3^- ions. The coordination geometry around Zn1 is distorted trigonal bipyrimidal with five nitrogen N atoms (N1, N2, N4, N5, N8) from one L^2 ligand and two azide anions, in which N2, N5, N8 atoms are the triangle plane, and N1 and N4 atoms at the apical positions. The ligand L^2 in **2** also presents the same coordination mode: μ_1-η^1:η^1:η^1, namely, which as a terminal tridentate ligand using the three nitrogen atoms (N1, N2, N4) on the same side of L^2 coordinates to one Zn^{2+} ion to form a 0-D discrete structure. The Zn–N bond distances are 1.950(4)–2.283(3) Å. And intermolecular hydrogen bonding C–H···Cl and π···π stacking interactions (Table S3†) resulting in 3-D supramolecular network with $3^6 \cdot 4^{13} \cdot 5^6 \cdot 6^3$ topology further stabilize crystal structure (Fig. 4).

$Zn_2(cis\text{-}L^3)X_4 \cdot S$. (X = Cl, S = H_2O for **3**; X = N_3, S = 0, for **5**). When the temperature of the reaction mixture was gradually elevated to 100 °C, two new complexes **3** and **5** with *in situ*

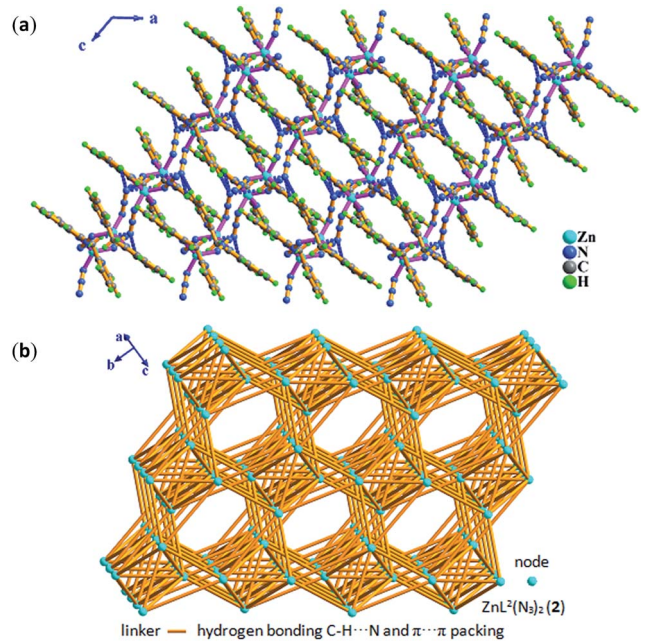

Fig. 4 In **2**, (a) 3-D supramolecular network assembled by intermolecular hydrogen bonding C–H···N and π···π packing interactions in *ac* plane. (b) 3-D $3^6\cdot4^{13}\cdot5^6\cdot6^3$ topology.

formed ring-forming and C–C coupling product L^3 from ligand L^2 and 2-pyridine formaldehyde were obtained as the two isologues. Both compounds **3** and **5** are 0-D dinuclear structures with monoclinic *P*2(1)/*c* space group.

As shown in Fig. 5, the molecule of **3** with a C_2 rotary axis contains two Zn(II) ions, one *in situ* formed ligand L^3, four terminal Cl^- ions and one lattice water molecule. Zn1 atom is penta-coordinated by three nitrogen atoms (N1, N2, N4) from the same ligand L^3 and two terminal chloride atoms (Cl1, Cl2) and presents a slightly distorted trigonal bipyrimidal coordination geometry. The ligand L^3, which adopts *cis*-conformation of four coordinated terminal groups referred to C6–C6a single bond and coordinates to two Zn^{2+} ions, shows μ_2-η^1:η^1:η^1:η^1:η^1:η^1 coordination mode. The Zn–N bond length of

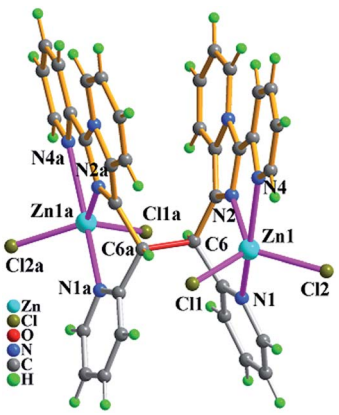

Fig. 5 Molecular structure of compound Zn_2(*cis*-L^3)$Cl_4\cdot H_2O$ (**3**) with atomic labels, and one lattice water molecule was omitted for clarity. The symmetric code: (a) 2 − *x*, *y*, 0.5 − *z*.

(2.030(9)–2.323(11) Å), and Zn–Cl (2.220(4)–2.278(5) Å) bond distances are in the range expected for this coordination geometry with zinc(II). Meanwhile, the existence of intermolecular hydrogen bonding C–H···Cl and π···π packing interactions (Table S3†) makes dinuclear molecular unit Zn_2(*cis*-L^3)Cl_4 to be linked into 1-D wave-like chain, and further assembled into 3-D network *via* inter-chain hydrogen bond C–H···O as shown in Fig. 6.

Compared with Cl^- ion, azide may have different spatial orientation, however compound **5** presents the same *P*2(1)/*c* space group. The molecule of **5** consists of two crystallographically independent Zn(II) ions showing a slightly distorted trigonal bipyrimidal coordination geometry, one *in situ* formed ligand L^3 with μ_2-η^1:η^1:η^1:η^1:η^1:η^1 coordination mode and four terminal η^1-N_3^- ions as depicted in Fig. 7. The Zn–N bond length of 1.955(5)–2.2.344(5) Å is consistent with that of complex **3**. Because of the hydrogen bonding C–H···N interactions from azide ion and pyridyl rings, each dinuclear molecular unit Zn_2(*cis*-L^3)$(N_3)_4$ links seven adjacent units to assemble into 3-D supramolecular network. If the dinuclear molecular unit Zn_2(*cis*-L^3)$(N_3)_4$ viewed as the node and the hydrogen bonding C–H···N interactions (Table S3†) as the linker, the resulting network can be simplified as $3^3\cdot4^{10}\cdot5^6\cdot6^2$ topology as displayed in Fig. 8.

[[Zn_2(*trans*-L^3)X_4]. (X = Cl for **4** and X = N_3 for **6**). When the reaction temperature finally rising to 120 °C, two complexes **4**

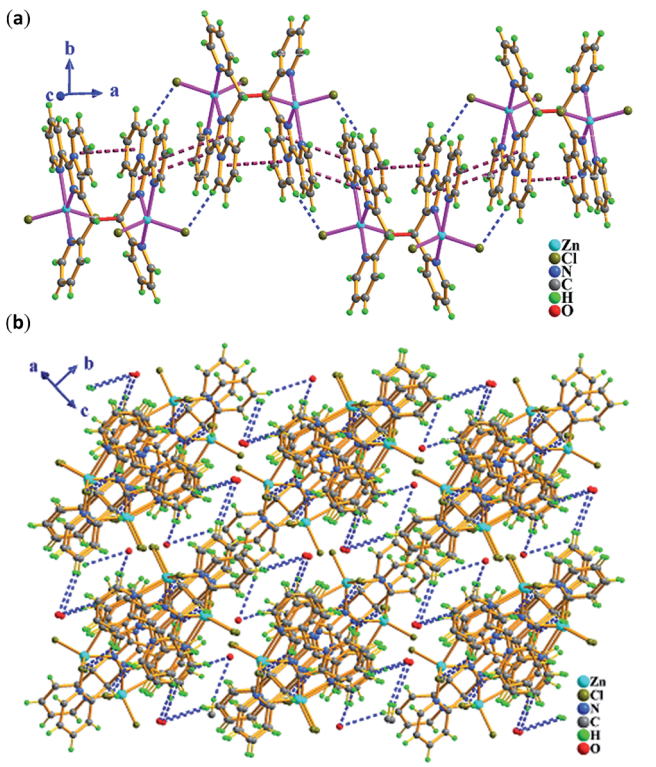

Fig. 6 In **3**, (a) 1-D wave-like chain constructed by inter/intra molecular hydrogen bonding C–H···Cl (blue dashed line) and π···π (plum dashed line) packing interactions along *a* axis. (b) 3-D supramolecular network assembled by interchain hydrogen bonding C–H···O (blue dashed line) interactions.

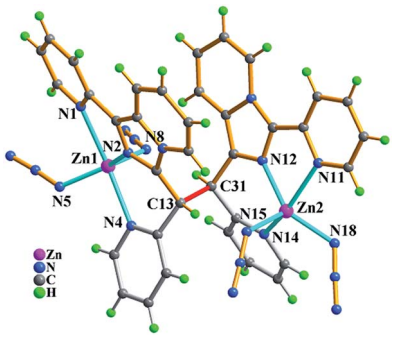

Fig. 7 Molecular structure of compound $Zn_2(cis\text{-}L^3)(N_3)_4$ (**5**) with partial atomic labels.

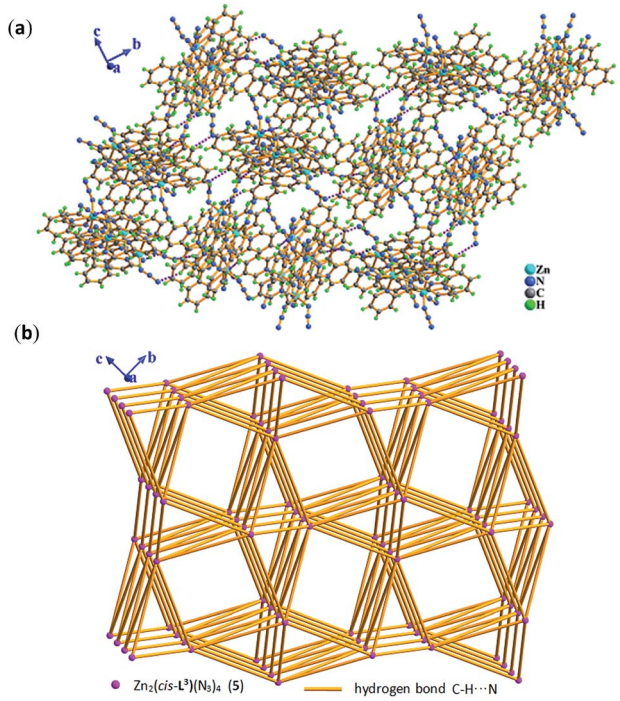

Fig. 8 In **5**, (a) 3-D supramolecular network assembled by intermolecular hydrogen bonding C–H···N interactions in *bc* plane. (b) 3-D $3^3\cdot4^{10}\cdot5^6\cdot6^2$ topological network constructed by inter/intra molecular hydrogen bonding C–H···N interactions in *bc* plane, where pink sphere represents dinuclear molecular unit $Zn_2(cis\text{-}L^3)(N_3)_4$ (**5**) and light orange stick represents intermolecular hydrogen bonding C–H···N interactions.

and **6** containing *in situ* formed L^3 were formed as the two isologues. Both compounds **4** and **6** are 0-D dinuclear structures with monoclinic $P2(1)/n$ space group for **4** and $P\bar{1}$ space group for **6**, respectively.

As shown in Fig. 9, the molecule of **4** possesses a crystallographically imposed inversion center located at the mid-point of C6–C6a single bond (blue color). Zn1 ion is pentacoordinated by three nitrogen atoms (N1, N2, N4) from the ligand L^3 and two terminal chloride atoms (Cl1, Cl2), demonstrating trigonal bipyrimidal coordination geometry similar to that of its conformational isomer **3**. One ligand L^3, which is

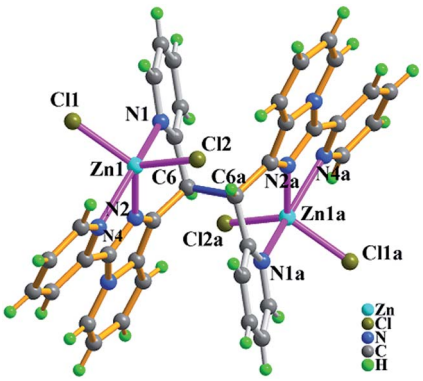

Fig. 9 Molecular structure of compound $Zn_2(trans\text{-}L^3)Cl_4$ (**4**) with partial atomic labels. The symmetric code: (a) $2-x, -y, 2-z$.

trans-conformation of four coordinated terminal groups referred to C6–C6a bond, coordinates to 2 equiv. of Zn^{2+} ions showing $\mu_2\text{-}\eta^1{:}\eta^1{:}\eta^1{:}\eta^1{:}\eta^1{:}\eta^1$ coordination mode. Meanwhile, the existence of intermolecular hydrogen bonding C–H···Cl interactions (Table S3†) makes dinuclear molecular $[Zn_2(trans\text{-}L^3)Cl_4]$ unit to be assembled into a 3-D supramolecular network with the topology of $3^5\cdot4^{18}\cdot6^5$ as shown in Fig. 10 and 11.

When Cl^- ion in complex **4** was completely replaced by azide ion, its isologues **6** was obtained. From Fig. 12, two zinc ions (Zn1 and Zn1a) in **6** have the same coordination pattern of

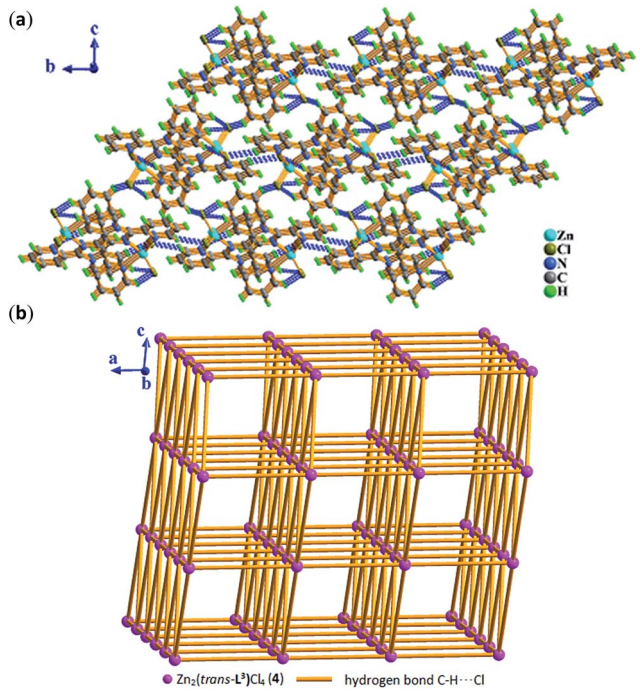

Fig. 10 In **4**, (a) 3-D supramolecular network assembled by intermolecular hydrogen bonding C–H···Cl interactions in *bc* plane. (b) 3-D $3^5\cdot4^{18}\cdot6^5$ topological network constructed by intermolecular hydrogen bonding C–H···Cl interactions in *ac* plane, where pink sphere represents dinuclear molecular unit $Zn_2(trans\text{-}L^3)Cl_4$ (**4**) and light orange stick represents intermolecular hydrogen bonding C–H···Cl interactions.

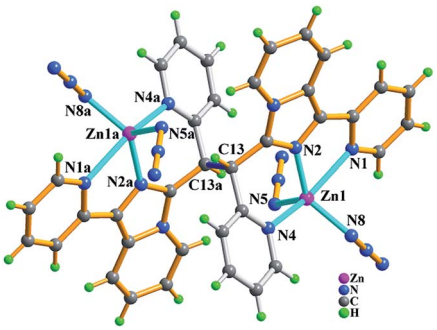

Fig. 11 Molecular structure of compound Zn_2(*trans*-L^3)$(N_3)_4$ (**6**) with partial atomic labels. The symmetric code: (a) 2 − *x*, −*y*, −*z*.

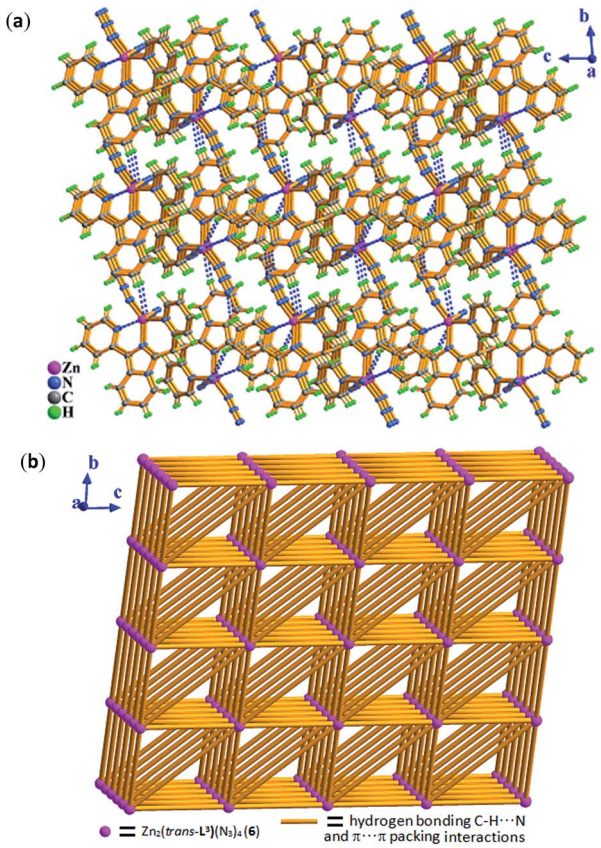

Fig. 12 In **6**, (a) 3-D supramolecular network assembled by inter-molecular hydrogen bonding C–H···N and π···π packing interactions in *bc* plane. (b) 3-D $3^4\cdot4^4\cdot6^{20}$ topological network constructed by inter-molecular hydrogen bonding C–H···N and π···π packing inter-actions in *bc* plane, where pink sphere represents dinuclear molecular unit Zn_2(*trans*-L^3)$(N_3)_4$ (**6**) and light orange stick represents intermo-lecular hydrogen bonding C–H···N and π···π packing interactions.

trigonal bipyrimidal coordination geometry as the zinc ions in **4.** Meanwhile, replacement of the azide ions have no effect on *trans*-conformation of the *in situ* formed L^2 ligand in **6.** It is to be observed that the varied spatial orientations of azide ions make the supramolecular structure of complex **6** different from that of complex **4**, exhibiting a 3-D supramolecular network with the topology of $3^4\cdot4^4\cdot6^{20}$ through intermolecular hydrogen bonding C–H···N and π···π packing interactions (Table S3†) as displayed in Fig. 12.

Structural *in situ* formation, transformation and temperature effect

In this contribution, the simple Schiff base ligand L^1 with a donor set of N_3 was firstly applied in the system of Zn-based aza-heterocyclic complexes. Initial reaction of $ZnCl_2$ at 80 °C with L^1 together with 2-pyridine formaldehyde afforded Zn-mono-nuclear compound ZnL^2Cl_2 (**1**) containing one *in situ* formed N-rich heterocycle L^2 with a donor set of N_3 *via* inter-molecular C–C/C–N coupling and ring forming reactions (Scheme S1†). And then two terminal coordinated Cl^- ions in **1** could be easily replaced by two N_3^- anions and produced the corresponding mononuclear zinc(II) compound $ZnL^2(N_3)_2$ (**2**). Increasing the reaction temperature to 100 °C, Zn^{2+}-induced intermolecular C–C coupling reaction between two L^2 molecules resulted in the formation of *cis*-conformation L^3 and the cor-responding Cl-based compound $[Zn_2(cis\text{-}L^3)Cl_4\cdot H_2O$ (**3**) as well as N_3-based substitute $[Zn_2(cis\text{-}L^3)(N_3)_4]$ (**5**). Continuing to increase the reaction temperature to 120 °C, *in situ* formed *cis*-L^3 can be lightly converted to the *trans*-L^3 and the corresponding Cl-based compound $Zn_2(trans\text{-}L^3)Cl_4$ (**4**) as well as N_3-based substitute $[Zn_2(trans\text{-}L^3)(N_3)_4]$ (**6**) with high thermal stability *via* the rotation of the C–C single bond derived by reaction temperature.

A careful inspection of experimental condition reveals that the reaction temperature has a significant contribution to final structures of two aza-heterocycles of L^{2-3} as well as six corre-sponding Zn-based compounds **1–6**, which might mainly depends on the influence of reaction temperature as reaction driving force. When reaction temperature is higher than 80 °C, the *ortho*-hydrogen atom of an imino group –CH=N–CH– in ligand L^1 can be markedly activated by the coordination induction of Zn^{2+} ion,[1,2] and pyridine as basic acceptor has the ability to deprotonate the imino carbon-bound α-position hydrogen atom and form 1,3-dipolar, leading to the occurrence of inter-molecular C–C/C–N coupling, [3+2] cycloaddition, transformation of *cis*/*trans*-isomers caused by C–C single rota-tion and formation of final Zn-imidazo[1,5-*a*]pyridine complexes L^2/L^3–Zn (Scheme S1†).

Fluorescence/UV absorption spectra and titration of L^1 + 2-Pfd

The luminescence properties of complexes **1–6** have been studied in the solid state at room temperature as depicted in Fig. S3.† Observably, **1–6** are blue emission with peak wave-lengths at the range from 428 to 450 nm. These emissions could be tentatively assigned as resulting from the ligand-to-metal charge transfer (LMCT).[5] Meanwhile, the fluorescence response of receptor L^1 towards Zn^{2+} was studied in 0.10 mM mixture solution of DMF and pyridine (volume ratio of 2 : 1) at the different temperatures. Upon excitation at 355 nm, L^1 and 2-pyridine formaldehyde (2-Pfd) (molar ratio of 1 : 1) in DMF and pyridine at 80–120 °C presented dark blue emission at 469 nm which could be attributed to the intra-ligand π–π* transition.[14] As stepwise addition of $ZnCl_2$ solution in DMF at 80 °C with

concentration ranging from 0.1 equiv. to 2.0 equiv., fluorescent emission of L^1 + 2-Pfd gradually red-shifted to 498 nm with their fluorescent intensity at 498 nm enhanced linearly with the Zn^{2+} concentration and saturated when [Zn^{2+}] reached to 1.00 equiv. (Fig. 13). Interaction between Zn^{2+} and L^1 + 2-Pfd was also studied by UV absorption spectra (Fig. S4†). Concomitant addition of $ZnCl_2$ into L^1 + 2-Pfd in DMF + pyridine causes a new absorption peak at 385 nm with intensity increased while that at 225, 261, 338, 430 nm decreased with four isosbestic points at 247, 272, 305, 348 nm. The binding ratio between Zn^{2+} and ligand was estimated to be 1 : 1 as confirmed by its job plot (Fig. S5†) and the related crystal structures.

As the temperature of the mixture [$ZnCl_2$ + L^1 + 2-Pfd] increased from 80 °C to 100 °C and 120 °C, the emission peak wavelength of the mixture $ZnCl_2$ + L^1 + 2-Pfd has an obvious red-shift to 525 nm for **3** (at 100 °C) and 531 nm for **4** (at 120 °C), respectively. The fluorescent intensity for **3** (Fig. S6†) and **4** (Fig. S7†) were both enhanced, but the peak shape were unchanged when compared to that at 80 °C (for **1**) due to the formation of 2D/3D dimensional supramolecular network assembled by a large number of intramolecular and intermolecular hydrogen bonding C–H···Cl and/or π···π stacking interactions.

The azide anion substitution effect of Cl-based Zn-compounds **1**, **3** and **4** was examined by fluorescence titration of **1**/**3**/**4** + NaN_3 at 80 °C, 100 °C and 120 °C, respectively (Fig. 14 and S8 and S9†). The fluorescence intensity of **1**/**3**/**4** + NaN_3 was, to some extent, enhanced with almost unchanged peak shape and position compared to the corresponding Cl-based Zn-compounds, in which the further enhanced fluorescence intensity of N_3-based Zn-compounds could be attributed to the stronger intermolecular/intramolecular hydrogen bonding interactions supported by more stable and higher dimensional supramolecular structures in the solid state.

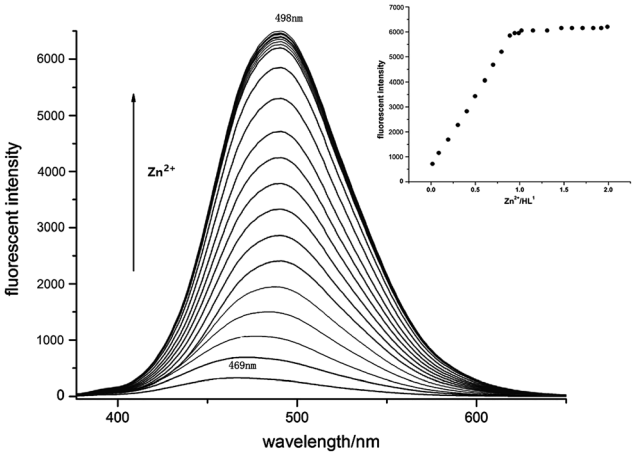

Fig. 13 Fluorescence emission spectra of L^1 + 2-Pfd upon addition of $ZnCl_2$ in DMF + pyridine. λ_{ex} = 355 nm at 80 °C ([L^1 + 2-Pfd] = 0.10 mM); [Zn^{2+}] = 0, 0.01, 0.02, 0.03, 0.04, 0.05, 0.06, 0.07, 0.08, 0.09, 0.10, 0.11, 0.12, 0.13, 0.131, 0.132, 0.133, 0.14, 0.15, 0.16, 0.17, 0.18, 0.19, 0.20 mM. (Inset: corresponding $ZnCl_2$ titration profile according to the fluorescence intensity, indicating 1 : 1 stoichiometry for Zn^{2+}/L^1 + 2-Pfd.)

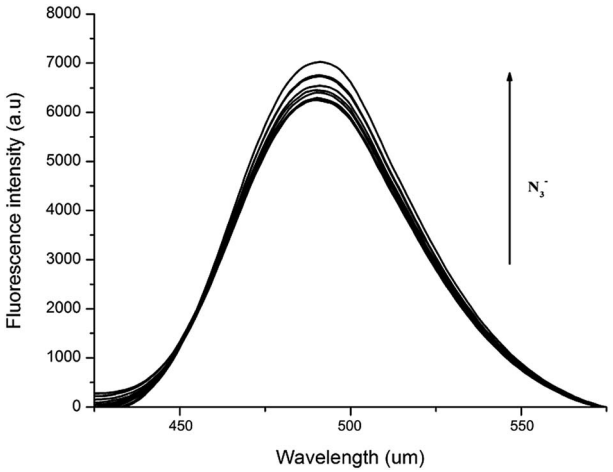

Fig. 14 Fluorescence emission spectra of **1** upon addition of NaN_3 in DMF + pyridine. λ_{ex} = 355 nm at 80 °C ([**1**] = 0.10 mM); [N_3^-] = 0, 0.01, 0.02, 0.03, 0.04, 0.05, 0.06, 0.07, 0.08, 0.09, 0.10, 0.11, 0.12, 0.13, 0.131, 0.132, 0.133, 0.14, 0.15, 0.16, 0.17, 0.18, 0.19, 0.20 mM.

In conclusion, this work describes the first example of efficient syntheses and complexation of two asymmetric N-rich heterocyclic ligands (L^{2-3}) containing imidazo-[1,5-*a*]-pyridine core involving solvothermal *in situ* ligand generation from simple tridentate N_3-set pyridine-type Schiff base ligand (L^1) mediated by Zn^{2+}. Further studies on *in situ* formation and conversion of ligands L^{1-3} and six corresponding Zn-complexes **1–6** show that temperature effect is the key factor rather than anion effect, which can tune their supramolecular connections and topologies of resulting zinc complexes. Obviously, this synthesis strategy may bring a broad interest in the construction of novel nitrogen-rich multidentate asymmetric heterocycles relating to metal ion induced α-H activation chemistry on imine bond –CH=N–, and relevant metal–organic frameworks as well as inorganic–organic hybrid materials with advanced luminescent and biological functions.

Acknowledgements

The authors are grateful for financial aid from the National Natural Science Foundation of P. R. China (Grant No. 21471061, 21671071 and 911220008), the Doctoral Program of Higher Education of China (Grant No. 20124407110007), Science and Technology Planning Project of Guangdong Province, Guangzhou, China (Grant No. 2013B010403024 and 2015B010135009) and the N. S. F. of Guangdong Province (Grant No. 2014A030311001 and C86186).

References

1 (*a*) S. M. Chiu, T. W. Wong, W. L. Man, W. T. Wong, S. M. Peng and T. C. Lau, *J. Am. Chem. Soc.*, 2001, **123**, 12720; (*b*) J. Xiang, W.-L. Man, S.-M. Yiu, S.-M. Peng and T.-C. Lau, *Chem.–Eur. J.*, 2011, **17**, 13044; (*c*) J. Xiang, W.-L. Man, J.-F. Guo, S.-M. Yiu, G.-H. Lee, S.-M. Peng, G.-C. Xu, S. Gao and T.-C. Lau, *Chem. Commun.*, 2010, **46**,

6102; (*d*) V. M. Aryuzina and M. N. Shchukina, *Khim. Geterotsikl. Soedin.*, 1968, **3**, 506; (*e*) M. P. Kochergin and V. A. Lifanov, *Khim. Geterotsikl. Soedin.*, 1994, **4**, 490; (*f*) M. E. Bluhm, M. Ciesielski, H. Görls, O. Walter and M. Döring, *Inorg. Chem.*, 2003, **42**, 8878.

2 (*a*) R. Huisgen, in *1,3-Dipolar Cycloaddition Chemistry*, ed. A. Padwa, John Wiley & Sons, New York, 1984, vol. 1; (*b*) D. H. Ess and K. N. Houk, *J. Am. Chem. Soc.*, 2008, **130**, 10187.

3 (*a*) B. A. Frazier, P. T. Wolczanski, I. Keresztes, S. DeBeer, E. B. Lobkovsky, A. W. Pierpont and T. R. Cundari, *Inorg. Chem.*, 2012, **51**, 8177; (*b*) B. A. Frazier, V. A. Williams, P. T. Wolczanski, S. C. Bart, K. Meyer, T. R. Cundari and B. Lobkovsky, *Inorg. Chem.*, 2013, **52**, 3295; (*c*) B. A. Frazier, P. T. Wolczanski, E. B. Lobkovsky and T. R. Cundari, *J. Am. Chem. Soc.*, 2009, **131**, 3428.

4 Y.-J. Ou, Z.-P. Zheng, X.-J. Hong, L.-T. Wan, L.-M. Wei, X.-M. Lin and Y.-P. Cai, *Cryst. Growth Des.*, 2014, **14**, 5339.

5 (*a*) H. A. Staab, *Angew. Chem., Int. Ed. Engl.*, 1962, **7**, 351; (*b*) J. Chang-Fong, K. Benamour, B. Szymonski, F. Thomasson, J.-M. Morand and M. Cussac, *Chem. Pharm. Bull.*, 2000, **48**, 729; (*c*) C. R. Sage, M. D. Michelitsch, T. J. Stout, D. Biermann, R. Nissen, J. Finer-Moore and R. M. Stroud, *Biochemistry*, 1998, **37**, 13893; (*d*) V. C. Sharma, L. Crankshaw and D. Piwnica-Worms, *J. Med. Chem.*, 1996, **39**, 3483; (*e*) H. Sakuta and K. Okamoto, *Eur. J. Pharmacol.*, 1994, **259**, 223; (*f*) G. J. Kant, J. L. Meyerhoff and R. H. Lenox, *Biochem. Pharmacol.*, 1980, **29**, 369.

6 (*a*) A. R. Katritzky, K. Suzuki and H.-Y. He, *J. Org. Chem.*, 2002, **67**, 3109; (*b*) M. Roy, B. V. S. K. Chakravarthi, C. Jayabaskaran, A. A. Karande and A. R. Chakravarty, *Dalton Trans.*, 2011, **40**, 4855.

7 (*a*) Y.-M. Chen, L. Li, Z. Chen, Y.-L. Liu, H.-L. Hu, W. Q. Chen, W. Liu, Y.-H. Li, T. Lei, Y.-Y. Cao, Z.-H. Kang, M.-S. Lin and W. Li, *Inorg. Chem.*, 2012, **51**, 9705; (*b*) C. Garino, T. Ruiu, L. Salassa, A. Albertino, G. Volpi, C. Nervi, R. Gobetto and K. I. Hardcastle, *Eur. J. Inorg. Chem.*, 2008, 3587.

8 G. M. Sheldrick, *SADABS, Version 2.05*, University of Göttingen, Göttingen, Germany.

9 G. M. Sheldrick, *SHELXS-97, Program for X-ray Crystal Structure Determination*, University of Göttingen, Göttingen, Germany, 1997.

10 G. M. Sheldrick, *SHELXS-97, Program for X-ray Crystal Structure Refinement*, University of Göttingen, Göttingen, Germany, 1997.

11 A. L. Spek, A Tool for the Calculation of the Disordered Solvent Contribution to the Calculated Structure Factors, *Acta Crystallogr., Sect. C: Struct. Chem.*, 2015, **71**, 9.

12 R. Huisgen, in *1,3-Dipolar Cycloaddition Chemistry*, ed. A. Padwa, John Wiley & Sons, New York, 1984, vol. 1.

13 (*a*) M. A. S. Goher, *Acta Chim. Hung.*, 1984, **117**, 215; (*b*) Z. Dori and R. F. Ziolo, *Chem. Rev.*, 1973, **73**, 247; (*c*) J. L. Manson, A. M. Arif and J. S. Miller, *Chem. Commun.*, 1999, 1479; (*d*) J. Ribas, M. Monfort, B. K. Ghosh and X. Solans, *Angew. Chem., Int. Ed. Engl.*, 1994, **33**, 2087; (*e*) X. Hao, Y. Wei and S.-W. Zhung, *Chem. Commun.*, 2000, 2271.

14 B. Bosnich, *J. Am. Chem. Soc.*, 1968, **90**, 627.